MST1 mutations in autosomal recessive primary immunodeficiency characterized by defective naive T-cell survival

Nadine T. Nehme[1,2], **Jana Pachlopnik Schmid**[1,2], **Franck Debeurme**[1,2], **Isabelle André-Schmutz**[1,2], **Annick Lim**[3], **Patrick Nitschke**[4], **Frédéric Rieux-Laucat**[1,2], **Patrick Lutz**[5], **Capucine Picard**[#2,6,7,8], **Nizar Mahlaoui**[#2,8], **Alain Fischer**[#1,2,8], and **Geneviève de Saint Basile**[#1,2,6,8]

[1]Inserm U768, Paris, France

[2]Université Paris Descartes, Sorbone Paris Cité, Faculté de Médecine, Necker Hospital, Paris, France

[3]Inserm U668 and Lymphocyte Development Unit, Institut Pasteur, Paris, France

[4]Service de Bioinformatique, Université Paris Descartes, Paris, France

[5]Unité d'Hématologie Pédiatrique, Hôpital de Hautepierre, Strasbourg, France

[6]Centre d'Etudes des Déficits Immunitaires, Assistance Publique–Hôpitaux de Paris (AP-HP) Hôpital Necker, Paris, France

[7]Inserm U980, Necker Medical Schoool, Paris, France

[8]AP-HP Hôpital Necker-Enfants Malades, Pediatric Immuno-Hematology Unit and National Referral Center for Primary Immune Deficiencies, Paris, France

[#] These authors contributed equally to this work.

Abstract

The molecular mechanisms that underlie T-cell quiescence are poorly understood. In the present study, we report a primary immunodeficiency phenotype associated with MST1 deficiency and primarily characterized by a progressive loss of naive T cells. The in vivo consequences include recurrent bacterial and viral infections and autoimmune manifestations. MST1-deficient T cells poorly expressed the transcription factor FOXO1, the IL-7 receptor, and BCL2. Conversely, FAS expression and the FAS-mediating apoptotic pathway were up-regulated. These abnormalities suggest that increased cell death of naive and proliferating T cells is the main mechanism underlying this novel immunodeficiency. Our results characterize a new mechanism in primary T-cell immunodeficiencies and highlight a role of the MST1/FOXO1 pathway in controlling the death of human naive T cells.

Introduction

The study of human T-cell primary immunodeficiencies has enabled the molecular characterization of many diseases caused by Mendelian inheritance of mutated genes[1-4] and has revealed the function of key molecules in T-cell biology. SCIDs are characterized by complete lack of T-cell development and, in some conditions, developmental blocks on other lymphoid lineages.[1,2] Several mechanisms can leads to faulty T-cell differentiation, such as the premature death of progenitor cells and impaired c-dependent cytokine signaling, VDJ recombination, or pre-TCR signaling.[1] In other forms of T-cell primary immunodeficiency, TCR-mediated T-cell activation is defective but T-cell differentiation is partially or fully preserved. The latter variously include deficiencies in DOCK8, ZAP-70, ITK, ORA1, and STIM-1, all of which are involved in the signaling cascade downstream of the TCR, and in molecules involved in the NF B pathway, such as NEMO and IKB .[2,5,6] These conditions are collectively referred to as combined immunodeficiencies (CIDs), because the functional consequences also include defective Ab production.

The molecular signatures of many more T-cell immunodeficiency phenotypes have yet to be identified. In the present study, we describe a new form of human CID observed in 4 patients from 2 families that is primarily characterized by a dramatically reduced pool of circulating naive T cells and impaired in vitro survival of the T-lymphocyte population. These patients were shown to carry homozygous mutations in the serine-threonine protein kinase 4 (*STK4*) gene, coding for the ubiquitously expressed mammalian sterile 20-like protein MST1.

Methods

Case reports

Patient F1P1 was born to a consanguineous family of Turkish origin (see Figure 1A). Since the age of 2, he had suffered from recurrent skin and lower respiratory tract infections caused by *Streptococcus pneumoniae* and *Haemophilus influenzae*, leading to bronchiectasis, recurrent perioral herpes simplex infections with positive anti–HSV1-2 IgG titer, *Varicella zoster* virus (VZV) infections, and extensive molluscum contagiosum. In addition, the patient had chronic EBV infection with persistent EBV viremia (53 000 copies/ mL at the age of 11 years) and positive anti–EBNA-1 and anti-VCA IgG Ab. At the age of 5, patient F1P1 was successfully treated for EBV+ Hodgkin B-cell lymphoma. The patient (now 17) is receiving Ig replacement therapy and anti-infective prophylaxis with antibiotics and antivirals. Apart from lymphocytopenia, his blood counts are consistently normal. A CT scan of the thymus performed at 11 years of age was normal in appearance, structure, and size compared with age-matched controls. He has no dysmorphic syndrome and his growth was within the normal range.

Family F2 is consanguineous and of Turkish origin, with 3 children affected (Figure 1A). Patients F2P1 and F2P2 developed recurrent bacterial infections and eczema-like lesions of the skin beginning in the first years of life, followed by recurrent pneumonitis and sinusitis associated with bronchiectasis. Recurrent herpes simplex stomatitis was noted. At the age of 2 years, patient F2P1 had an episode of neutropenia (associated with antinuclear and anticardiolipin Abs) that was treated with steroids and azathioprine until the age of 7. Persistent EBV viremia (9000 copies/µg total DNA at the age of 9 years old) associated with detection of IgG Ab to EBNA-1 and VCA was noted and was transiently accompanied by neutropenia. F2P1 developed EBV B-cell–lymphoproliferative syndrome with multiple locations that was temporarily controlled by anti-CD20 Ab therapy. She underwent hematopoietic stem cell transplantation (HSCT) from an unrelated donor and died from

GVHD and infectious complications 6 months later. Patient F2P2 also developed autoimmune hemolytic anemia at the age of 1 year and displayed persistent EBV viremia (12 000 copies/mL at the age of 10 years) since that time. She was treated with anti-CD20 Abs at the age of 11 and underwent HSCT (with her mother as donor) at the age of 14.5 years. Persistent GVHD and infections led to death 5 months later.

Patient F2P3 had mild erythematous skin lesions and molluscum contagiosum beginning in the first year of life. She was not infected with EBV and after the initiation of prophylactic Ig and antibiotic therapy, no other complications occurred until she received a T cell–depleted HSCT from her haploidentical mother at the age of 4 years. Two years later, the HSCT appears to have cured the immunodeficiency. At the age of 5, patient F2P3 was found to have tricuspid valve insufficiency, together with moderate right ventricular hypertrophy that has not progressed since then. Patients F2P1, F2P2, and F2P3 did not display dysmorphic symptoms and grew normally.

All patients and their parents gave their informed consent to participate in the study in accordance with the Declaration of Helsinki. Data collection and genetic studies were approved by the local independent ethics committee and the French Advisory Committee on Data Processing in Medical Research.

SNP analysis and sequence analysis

Single nucleotide polymorphism (SNP) and sequence analysis were as described previously.[7] Primers are listed in supplemental Table 1 (available on the *Blood* Web site; see the Supplemental Materials link at the top of the online article).

Gene expression analysis

Gene expression assays were performed as described previously.[7] RT-PCR was performed on each sample using *MST1*-specific primers (supplemental Table 1). For comparative, real-time RT-PCR assays, ACTB (Hs99999903), MST1 (Hs00178979), BCL2L11 (Hs01083836), BCL-2 (Hs99999018), and KLF2 (Hs00360439) probes were labeled with 6-carboxy-fluorescein dye (Applied Biosystems). The data were analyzed using the comparative threshold cycle method and are presented as the relative change in gene expression normalized against the calibrator sample corresponding to control T cells.

Cells and cultures

PBMCs were isolated from blood samples taken from MST1-deficient patients and controls. The MST1-deficient patients carried a homozygous deletion or a homozygous nonsense mutation in *MST1* with a predicted early (F1P1-MST1: R117X) or late (F2P1-F2P2-F2P3-MST1: T1193fsX369) premature stop codon. Phorbol 12-myristate 13-acetate (PMA)/ionomycin-induced T lymphoblasts were obtained by incubating PBMCs for 72 hours with PMA (40 ng/mL; Calbiochem), ionomycin (10^{-5} M; Calbiochem), and IL-2 (40 IU/mL; Novartis) in Panserin medium (Biotech) supplemented with 10% human AB serum (Etablissement Français du Sang). More IL-2 (100 IU/mL) was added the cells were then cultured for 20 days in Panserin medium with 5% human AB serum.

Immunoscope analysis

The SNP and sequence analysis were performed as described previously.[8]

Protein blots

Cell extracts and protein blots were prepared as described previously.[7] Abs against MST1 (Ab recognizing the aminoterminal region of human Mst1 protein), FOXO1, BCL2, and

actin are described in supplemental Table 2. The intensity of the immunoblot bands was quantified using ImageJ Version 1.4.3.67 Launcher Symmetry software.

Flow cytometry

Abs were purchased from eBioscience or BD Pharmingen; clone identifiers are listed in supplemental Table 2. Standard flow cytometry methods were used for staining cell-surface markers. Data were collected on a FACSCanto II Version 6.1 (BD Biosciences) and analyzed with FlowJo Version 8.8.4 software (TreeStar). Fluorescence intensities were quantified across experiments by normalizing the mean values obtained for each patient against the mean values obtained for a control (set as 100%) in each experiment or time point.

Apoptosis assay

The apoptosis assay was performed as described previously.[9] Briefly, PMA/ionomycin blasts were stimulated with 5-100 ng/mL of anti-CD95 Abs (APO-1.3).

Proliferation assays and cell-cycle analysis

Patient and control PBMCs (purified by density gradient centrifugation) were cultured in medium alone or in the presence of PHA (5 μg/mL) for 3 days in the presence of OKT3 (50 ng/mL) or ionomycin (10^{-5}M) and PMA (10^{-7}M) for 4 days or with Ags such as *Candida* (50 μg/mL; Bio-Rad), tetanus toxoid (0125 lf/mL; Statens Serum Institute), and VZV (Virion Institute, VZV 1191) for 6 days. [^{3}H] thymidine was added for the last 18 hours. Cell proliferation was determined as cpm of [^{3}H] thymidine incorporation.

Cell proliferation was monitored by labeling T cells with 10μM CFSE (Invitrogen) before stimulation with PMA/ionomycin according to the manufacturer's instructions. Every 24 hours, cells were harvested and the CFSE dilution was assessed by flow cytometry.

Cell proliferation and cell-cycle analysis were determined by measuring the incorporation of the nucleoside analog 5-ethynyl-2 -deoxyuridine (EdU) into newly synthesized DNA, according to the manufacturer's instructions (Click-iT EdU; Invitrogen). EdU incorporation was measured by the abundance of a fluorescent product and sized on a FACSCanto flow cytometry system (BD Biosciences) running FlowJo Version 8.8.4 software (TreeStar).

Detection of apoptotic cells with annexin V

The proportions of apoptotic, dead, and viable cells were determined using the annexin V-PE Apoptosis Detection Kit I (BD Biosciences) according to the manufacturer's instructions. Cell fluorescence was measured analyzed on the FACSCanto system running FlowJo Version 8.8.4 software.

Transwell migration assay

Chemotaxis assays using a 24-well Transwell (Costar; Corning) were performed as described previously.[10] Briefly, 5×10^5 PBMCs were loaded into the upper chamber and allowed to transmigrate into the lower chamber containing either 100 ng/mL of CCL19 (R&D Systems), 100 ng/mL of CCL21 (R&D Systems), a 1:1 mixture of the 2 chemokines, or 1 μg/mL of SDF 1 for 3 hours at 37°C in 5% CO_2. The cells that migrated to the lower chamber were stained with cell-surface Abs for flow cytometry analysis. The percentage migration was calculated by dividing the number of cells in the lower chamber by the total cell input and multiplying the result by 100. Ratios were calculating according to the initial number of CD4$^+$ T cells for each individual. Chemotaxis data represent the average of triplicate wells in duplicate experiments.

Accession codes

The GenBank reference sequence for *MST1* mRNA is NM_006282. The Protein Databank reference sequence for peptide MST1 is NP_006273.1.

Statistics

Results are expressed as the means ± SD. Statistical analysis was performed using a 2-tailed, unpaired Student *t* test. The threshold for statistically significance was set to *P* < .05.

Online supplemental material

Supplemental Figure 1 shows the immunoscope analysis of the TCR Vb repertoire of 2 patients. Supplemental Figure 2 shows the result of multipoint LOD scores analysis plotted along chromosome 20 containing the *MST1* gene. Supplemental Figure 3 shows the impaired expression of CD127, CCR7, and CD62L by Mst1-deficient T cells, contrasting to the normal expression of CD132. Supplemental Figure 4 shows impaired in vitro chemotaxis of MST1–deficient CD4 T cells to CCL19 and CCL21 chemokines compared with normal migration in response to SDF1. Supplemental Figure 5 shows the increase expression of Fas (CD95) at the surface of MST1-deficient T cells. Supplemental Table 1 lists the primers used to sequence Mst1 genomic DNA, and supplemental Table 2 lists the Abs and labeled proteins used in this study.

Results

MST1 mutations are associated with a progressive T-cell immunodeficiency

We studied 2 consanguineous unrelated families from Turkey in which 4 individuals had been diagnosed with CIDs (Figure 1A and Table 1). All 4 presented with recurrent bacterial and viral infections, autoimmune manifestations, dermatitis, hypergammaglobulinemia G and A, and contrasting, defective Ab responses (Table 1). Immunophenotyping with flow cytometry revealed that all patients had progressive CD4 T-cell lymphopenia (Table 1) characterized primarily by profoundly low naive CD4 T-cell counts (Table 1 and Figure 1B). The frequency of CD8 T cells was close to that of age-matched controls (Table 1). However, when subsets of CD8 T cells were enumerated in 2 cases, a dramatic reduction in naive (CD45RA$^+$CCR7$^+$) CD8$^+$ T cells (Table 1) was observed together with a lesser decrease in memory (CD45RA$^-$CCR7$^-$) CD8 T cells (data not shown). In one patient (F2P2), 80% of the CD8 population expressed an effector-memory phenotype (CD45RA$^+$CCR7$^-$RIL-7$^-$), likely reflecting an in vivo expansion of this population in a context of chronic viral infection. It is noteworthy that a fraction of the T cells expressed HLA class II molecules, which is an indication of in vivo activation (Table 1). The patients' B-cell counts were somewhat low, but their natural killer cell counts were normal (Table 1). Immunoscope analysis of T lymphocyte TCR V / usage revealed an abnormal profile with a small number of peaks; this indicates restricted heterogeneity of TCR usage and/or clonal expansion (supplemental Figure 1). The number of regulatory T cells, as assessed by Foxp3$^+$CD25^{hi}CD4$^+$ coexpression, in 3 patients was decreased because of overall CD4 T-cell lymphopenia but was proportionally normal (Table 1).

Known causes of CIDs were excluded by genetic analysis (data not shown). To determine the genetic basis of the immune disorder in these families, we screened for homozygous chromosomal regions by performing a genome-wide SNP analysis of DNA from all 4 patients and their relatives (Figure 1A). This analysis revealed a single region of 5.5 Mb on chromosome 20q13.12 compatible for all markers with a multipoint analysis LOD score of 3.8 (supplemental Figure 2). Of the region's 74 genes, 5 candidate genes were sequenced prioritizing genes susceptible to being involved in the hematopoietic system; of them, *STK4/ MST1* appeared to be an interesting candidate because it is known to be expressed in the

lymphoid tissues and because its deficiency impairs T-cell function in mice.[11] *STK4* was the only gene harboring mutations in patients.

Nucleotide sequencing of *MST1* revealed a putative truncation mutation in all 4 patients. One patient (F1P1) carries a homozygous 349C > T nucleotide change in exon 4, resulting in a R117X nonsense codon (Figure 1C). The 3 affected individuals from the second family (patients F2P1, F2P2, and F2P3) carry a homozygous, single-nucleotide deletion (T1103 del), which creates a frameshift mutation at residue 368 and an immediately contiguous nonsense codon (369X; Figure 1C). In both families, the parents and siblings were found to be heterozygous for the mutated *MST1* allele. The R117X mutation in family 1 affects the protein kinase domain, whereas the 369X transition in family 2 is located in MST1 regulatory domain downstream of the caspase3 cleavage site and upstream of the Salvador/Rassf/Hippo (SARAH) domain[12,13] (Figure 1C). These alleles are absent from ethnically matched controls, dbSNP, and the 1000 Genomes Project database.

MST1 expression

We next analyzed the MST1 expression pattern using quantitative real-time PCR on a panel of cDNAs from a wide range of hematopoietic and nonhematopoietic tissues (Figure 2A). MST1 was found to be ubiquitously expressed in all tested tissues, with the highest levels in hematopoietic tissues such as leukocytes and spleen. In the mouse, it has been reported that the MST1 polypeptide and mRNA are 10-fold less abundant in wild-type effector/memory $CD4^+$ T cells than in wild-type naive $CD4^+$ T cells.[11] To determine whether MST1 is similarly regulated in humans, we used quantitative, real-time PCR to analyze *MST1* expression in naive and effector/memory CD4 and CD8 T-cell subpopulations from healthy controls (Figure 2B). The abundance of *MST1* mRNA in control effector/memory CD4 and CD8 T cells was half that observed in control naive CD4 and CD8 T cells (Figure 2B).

We next assessed the impact of *MST1* nonsense mutations on the expression of *MST1* mRNA and protein in patients' lymphocytes. *MST1* mRNA transcript expression was much lower in MST1-deficient T cells than in control T cells (Figure 2C). MST1-mutated proteins were not detected in cell lysates from patients F1P1 or F2P3 relative to lysates from controls or heterozygous subjects (Figure 2D). MST1 can be cleaved by caspases and the cleaved form translocates to the nucleus.[14] Because the mutation identified in F2 patients is located downstream of the caspase 3 cleavage sites, it could still lead to the generation of a caspase-cleaved active MST1 fragment constitutively present in the nucleus. Therefore, we assessed the expression of the MST1 aminoterminal protein fragment in nuclear lysates of the patients' lymphoblasts. MST1 protein was not detected in the cytoplasmic fraction or in nuclear lysates (data not shown). These data indicate that this newly observed immunodeficiency is associated with recessive, loss-of-function/expression mutations in the *MST1* gene.

Impaired proliferation and survival of MST1-deficient T cells

MST1-deficient patients had CD4 T-cell lymphopenia and markedly reduced naive T-cell counts (Figure 1B). To further characterize the peripheral T-cell deficiency observed in MST1-deficient patients, we assessed the proliferation response of the patients' T cells to several stimuli. The MST1-deficient T cell proliferation responses to Ags such as Candida, tetanus toxoid, and VZV and mitogens such as anti-CD3 Ab or PHA were markedly impaired (Table 1). Combination of PMA and ionomycin with IL-2 supported weak T-cell proliferation (Table 1). It is noteworthy that T cells from the youngest patient (F2P3) had detectable Ag-stimulated proliferation activity (Table 1).

To further investigate the proliferation potential of MST1-deficient T cells, we labeled control and MST1-deficient PBMCs with CFSE before PMA/ionomycin stimulation and sequentially assessed CD4 and CD8 T-cell proliferation by CFSE dilution. At day 1, there was no difference between the CFSE profiles of control and MST1-deficient CD4 and CD8 T cells (Figure 3A). At day 3, most of the control CD4 and CD8 T cells had divided, as indicated by a decrease in CFSE fluorescence (Figure 3A top). In contrast, a significant proportion of the MST1-deficient CD4 and CD8 T cells still retained the dye, indicating that these cells either had not divided or were dead (Figure 3A bottom). To test the latter possibility, we examined apoptosis of the dividing T cells (based on the ability to bind annexin V coupled to CFSE staining). At all tested time points (days 1-5, Figure 3B), the proportion of annexin V$^+$ cells was markedly higher in the MST1-deficient T cells than in control T cells. This was confirmed by the absolute cell counts (Figure 3C). The MST1-deficient T cells exhibited a high apoptosis rate and thus a dramatic decrease in cell numbers between days 1 and 3 (Figure 3C). In contrast to control T cells, MST1-deficient T cells showed a persistently high rate of apoptosis over time (Figure 3B). The few MST-deficient annexin V$^-$ CD4 and CD8 T cells showed no CFSE dilution at day 3 and a limited dilution at day 4 (Figure 3D bottom), whereas control CD4 and CD8 annexin V$^-$ T cells had undergone 2 or more divisions (Figure 3D top). A low but significant peak of dividing MST1-deficient T cells was repeatedly observed at day 1 (Figure 3D arrow), but not at later time points. These data indicate that MST1 is essential for T-cell survival and that the overall reduction of the number of dividing MST1-deficient T cells is essentially the consequence of an accelerated apoptosis.

Further confirmation of the MST1-deficient CD4 T cells' major impairment in proliferation relative to control CD4 T cells was provided by the low fraction of cells in the S phase (as measured by EdU incorporation) and an accumulation of those in the G_1 phase (Figure 3E-F top). Similarly, MST1-deficient CD8 T cells proliferated less than control CD8 T cells (Figure 3E-F bottom). These data suggest that in addition to MST1's role in T-cell survival, the protein could play a role in cell-cycle progression and therefore T-cell proliferation.

The molecular consequences of MST1 deficiency

Given that the transcription factor Foxo1 is reportedly activated by Mst1,[15] and considering the critical function of Foxo1 in T cells homeostasis,[16,17] we investigated whether the FOXO1 protein expression level was affected in MST1-deficient T cells. Indeed, FOXO1 protein levels were much lower in patient cell lysates than in control and heterozygous cell lysates (Figure 4A). These data indicate that the interaction between MST1 and FOXO1 is necessary for FOXO protein stability and expression in T cells.

In the mouse, Foxo1 has been found to control Il7R expression in naive T cells.[17] Therefore, we analyzed the T-cell surface expression of IL-7R on various PBMC subsets. Compared with control naive CD4 T cells, MST1-deficient naive CD4 CD45RA$^+$ T cells expressed significantly subnormal amounts of IL-7R (CD127) protein (Figure 4B and supplemental Figure 3A left). IL-7R expression was also much lower on effector/memory CD4 CD45RO$^+$ T cells and absent on CD8 T cells (Figure 4B and supplemental Figure 3A right). In contrast to the low expression of IL-7R on MST1-deficient T-cell subpopulations, expression of CD132 (the -chain receptor subunit of IL-7R that is shared with other cytokine receptors) was not affected by the MST1 deficiency (Figure 4C and supplemental Figure 3B). These observations reveal a critical, specific role for MST1 in the control of IL-7R expression. We were able to determine in vitro proliferation in the presence of IL-7 once (with T cells from patient F1P1), but adjunction of this interleukin did not enable cells to survive, as measured by cell counts (data not shown).

Several studies in mice have reported that Foxo1 controls the expression of L-selectin (CD62L) and the C-C chemokine receptor type 7 (CCR7), 2 important homing receptors expressed on naive CD4 and CD8 T cells.[16,17] We therefore examined the expression of CCR7 and CD62L on T cells isolated from control and MST1-deficient patients. There was a consistent reduction in CCR7 expression in all MST1-deficient T-cell subpopulations relative to levels in control T cells (Figure 4D and supplemental Figure 3C). Further analysis of homing receptors revealed that CD62L expression was also dramatically lower in the patients' naive CD4 CD45RA^{+} T cells than in control CD4 CD45RA^{+} T cells (Figure 4E and supplemental Figure 3D), as well as in the patients' effector/memory CD4 CD45RO^{+} T cells (Figure 4E). Both L-selectin and CCR7 expression are dependent on the activation of the transcription factor Kruppel-like factor 2 (KLF2),[18] through direct binding of FOXO1 to the KLF2 promoter.[19] We therefore examined KLF2 mRNA expression in MST1-deficient T cells. The assay results revealed markedly lower KLF2 mRNA expression in PBMCs from MST1-deficient patients than in control PBMCs (Figure 4F). The difference in lymphocyte subsets between control and patient PBMCs may also account for the difference in the level of transcript expression. These data show that MST1 deficiency leads to impaired expression of the homing receptors CCR7 and CD62L and likely in the transcription factor KLF2. These defects could impair naive T-cell homing to secondary lymphoid organs, because the chemotactic response to CCL19/CCL21 was impaired in vitro (supplemental Figure 4).

MST1 deficiency is associated with increased FAS membrane expression and FAS-induced apoptosis of T cells

The occurrence of massive apoptosis in freshly isolated MST1-deficient T cells (Figure 5A left) and in response to stimulation with PMA/ionomycin in vitro (Figure 3B), the progressive lymphopenia, and the major loss of naive CD4 cells observed in vivo suggested that naive T cells may undergo apoptosis after repetitive exogenous stimulations or when exposed to stress signals. To further investigate MST1's function in T-cell apoptosis, we investigated the protein's potential role in the control of the death-receptor–induced apoptotic pathway by determining the sensitivity of MST1-deficient and control PMA/ionomycin–activated lymphoblasts to FAS-mediated apoptosis. At doses of the anti-CD95 (FAS) Ab Apo1.3 up to 20 ng/mL (Figure 5A right), MST1-deficient lymphoblasts showed significantly higher apoptosis levels than those observed in control T cells. Remarkably, all MST1-deficient T-cell subsets expressed significantly higher amounts of surface FAS than did control T cells (Figure 5B and supplemental Figure 5). In particular, FAS expression was very high in MST1-deficient naive CD4 CD45RA^{+} T cells compared with the low levels seen in the corresponding control cells (Figure 5B and supplemental Figure 5). These data show that FAS expression is up-regulated at the surface of MST1-deficient T cells and can trigger cell apoptosis after cell activation.

Because IL-7R signaling induces BCL2 expression,[20] we investigated whether MST1 deficiency, which is associated with low IL-7R expression, impairs BCL2 expression. Indeed, *BCL2* mRNA expression, as monitored by quantitative PCR, was found to be 3- to 5-fold lower in MST1-deficient PBMCs (from F2P2 and F1P1, respectively) than in control cells (Figure 5C). This relative decrease in *BCL2* mRNA expression level was correlated with low BCL2 protein expression in MST1-deficient PBMC lysates compared with controls (Figure 5D). These data indicate that MST1 is required to maintain BCL2 expression and the survival of T cells in vivo.

These data highlight the impaired survival of MST1-deficient T cells with an increase in cell apoptosis that is probably related to defective IL-7R signaling and increased FAS expression/signaling.

Discussion

The present study reports a new primary T-cell immunodeficiency associated with homozygous loss of function/expression of the *MST1*-encoding gene, as observed in 4 patients from 2 families. Direct demonstration that *MST1* mutations were causal could not be provided, because the patient cells did not survive attempted in vitro complementation of the defect. However, the presence of nonsense mutations, the defective expression of both *MST1* mRNA (probably via nonsense-RNA–mediated decay) and protein, and the phenotype's similarity to that of the *mst1*^{−/−} mouse all argue in favor of a causal link between MST1 deficiency and the expressed immunodeficiency. Remarkably, and although MST1 is ubiquitously expressed and has been shown in mice to be involved in heart muscle size (at least),[21] no extralymphocytic defects were apparent. Possible functional redundancy with MST2 function[22,23] may account for this observation. As observed in mice, MST1 expression was highest in the patients' naive T cells, a finding that strongly suggests that MST1 has major role in this T-cell subset.

MST1 was first described in *Drosophila* as part of the Hippo tumor-suppressor pathway[24-26] that induces the transcriptional coactivation of target genes involved in cell proliferation and survival.[24] The amino acid sequence of MST1 is highly conserved in humans and mice. The serine-threonine kinase MST1 contains an N-terminal catalytic domain, an autoinhibitory segment, and a C-terminal coiled-coil SARAH domain that mediates hetero- and homodimerization.[27] MST1 is known to be involved in several pathways controlling cell death,[27-30] and its activity can be regulated by caspase-induced cleavage, prompting translocation to the nucleus and interaction with other proteins. In murine lymphocytes, the physiologic role of mst1 consists primarily of promoting the survival and quiescence of naive T cells,[11,31] egress from the thymus, and homing to lymphoid organs.[10,32] Indeed, mst1^{−/−} mice display an accumulation of mature lymphocytes in the thymus, loss of naive T cells, and depletion of lymphoid organs. In humans, the MST1-FOXO1 activation pathway likely mediates these functions, at least in part. The FOXO transcription factors represent one of several classes of functionally relevant MST1 substrates.[17,33,34]

Our present findings show that MST1 also has a key role in the maintenance and homing of human naive T cells. The importance of the role of MST1 in cell survival is emphasized by the severe in vivo loss of naive T cells (both CD4 and CD8 T cells) over time and the dramatic in vitro cell death of activated cells. Defective expression of IL-7R and anti-apoptotic BCL2 molecules may account for this finding (at least in part). MST1 deficiency also results in loss of FOXO1, a pivotal intermediate in the defective expression of IL-7R, the homing receptors CCR7 and CD62L, and their triggering transcription factor KLF2.[16,18,19] In addition, the increased number of CD8 T cells (but not CD4) with low expression of IL-7R, CCR7, and CD62L associated with high expression of Fas evidenced in 1 patient may also reflect the expansion of "exhausted" (or terminally differentiated) effector-memory T cells in the context of chronic viral infections.[35,36] The restricted TCR repertoire observed in Mst1-deficient patients likely reflects the expansion of a limited number of effector clones in this environmental context. MST1 deficiency may also impair the development and/or maintenance of regulatory T cells, the absolute number of which was decreased in the patients, an observation that might be related to the advent of autoimmune manifestations in 2 patients. Naive T cells from mst1^{−/−} mice were reported to proliferate strongly in response to TCR/CD3 stimulation. Unfortunately, we were unable to test or confirm this result when using T cells isolated from MST1-deficient patients because most of them (3 of 4) had no more naive T cells in the periphery. Interestingly, T cells isolated from the youngest patient still harboring a low number of naive T cells exhibited a detectable proliferation after PMA/ionomycin and Ag stimulation.

It has been proposed recently that naive T-cell quiescence in mice is an active phenomenon based on the balance between Foxo1 and Foxp1 transcription factor activities.[37] In contrast to Foxo1, Foxp1 down-regulates IL-7R expression. An MST1 deficiency would lower FOXO1 expression and allow the activity of FOXP1 to continue unimpeded. Cytokine-based or TCR triggering is likely to induce T-cell activation at a lower threshold in this context because the MST1-based barrier to activation is no longer present. In this respect, our findings that MST1-deficient naive T cells overexpress FAS and exhibit an early, transient peak (day 1) of proliferation ex vivo are consistent with in vivo activation of the naive T-cell pool in the absence of MST1. This activation state may contribute to cell death through increased FAS-mediated apoptosis, as seen here, although other cell death pathways may have a role. It remains to be seen whether the observed premature cell death of naive T cells is also related to MST1-induced changes in the expression of SOD2 and catalase-2 enzymes that neutralize the reactive oxygen species generated by cell stress.[38,39] It is therefore conceivable that MST1 plays a central, orchestrating role in maintaining naive T cells by preventing the activation of a range of cell death pathways.

The present study describes a new primary T-cell immunodeficiency with fairly severe phenotypic consequences that are characterized by recurrent bacterial and viral infections and autoimmune manifestations. Faulty control of EBV replication is a constant feature in B-cell lymphoproliferation and Hodgkin lymphoma, as observed in other severe forms of T-cell immunodeficiency.[40,41] Therefore, the mechanism underlying the defective maintenance of naive T cells in MST1 deficiency probably differs from those described in known impairments in T-cell differentiation (eg, c, JAK3, Rag-1, Rag-2, and Artemis deficiencies)[1,2] or T-cell activation (eg, ZAP-70, ORA-1, STIM-1, ITK, or DOK-8 deficiencies).[1,2,5,42] MST1 deficiency phenotype shares similar findings with DOCK8 deficiency, which include susceptibility to viral infections, T-cell lymphopenia, and reduced in vitro T-cell proliferation.[5,43-45] Nevertheless, there are also significant phenotypic differences that predominantly consist in reduced naive CD8 T-cell counts, preserved CD4 T-cell proliferation, eosinophilia, and marked atopy that are observed in DOCK8 deficiency only.[43] Furthermore, it may be that other T-cell immunodeficiencies characterized by a selective reduction in the naive T-cell subset will help to determine the roles of other important molecules required for human T-cell maintenance and control of viral replication and reactivity to self.

Acknowledgments

References

1. Fischer A. Human primary immunodeficiency diseases. Immunity. 2007; 27(6):835–845. [PubMed: 18093537]

2. International Union of Immunological Societies Expert Committee on Primary Immunodeficiencies. Notarangelo LD, Fischer A, Geha RS, et al. Primary immunodeficiencies: 2009 update. J Allergy Clin Immunol. 2009; 124(6):1161–1178. [PubMed: 20004777]

3. Chinen J, Shearer WT. Advances in basic and clinical immunology in 2010. J Allergy Clin Immunol. 2011; 127(2):336–341. [PubMed: 21281863]

4. Schuetz C, Niehues T, Friedrich W, Schwarz K. Autoimmunity, autoinflammation and lymphoma in combined immunodeficiency (CID). Autoimmun Rev. 2010; 9(7):477–482. [PubMed: 20146941]

5. Zhang Q, Davis JC, Lamborn IT, et al. Combined immunodeficiency associated with DOCK8 mutations. N Engl J Med. 2009; 361(21):2046–2055. [PubMed: 19776401]

6. Feske S. CRAC channelopathies. Pflugers Arch. 2010; 460(2):417–435. [PubMed: 20111871]

7. Côte M, Menager MM, Burgess A, et al. Munc18-2 deficiency causes familial hemophagocytic lymphohistiocytosis type 5 and impairs cytotoxic granule exocytosis in patient NK cells. J Clin Invest. 2009; 119(12):3765–3773. [PubMed: 19884660]

8. Lim A, Baron V, Ferradini L, Bonneville M, Kourilsky P, Pannetier C. Combination of MHC-peptide multimer-based T cell sorting with the Immunoscope permits sensitive ex vivo quantitation and follow-up of human CD8+ T cell immune responses. J Immunol Methods. 2002; 261(1-2):177–194. [PubMed: 11861076]

9. Rieux-Laucat F, Blachere S, Danielan S, et al. Lymphoproliferative syndrome with autoimmunity: a possible genetic basis for dominant expression of the clinical manifestations. Blood. 1999; 94(8):2575–2582. [PubMed: 10515860]

10. Dong Y, Du X, Ye J, et al. A cell-intrinsic role for Mst1 in regulating thymocyte egress. J Immunol. 2009; 183(6):3865–3872. [PubMed: 19692642]

11. Zhou D, Medoff BD, Chen L, et al. The Nore1B/Mst1 complex restrains antigen receptor-induced proliferation of naive T cells. Proc Natl Acad Sci U S A. 2008; 105(51):20321–20326. [PubMed: 19073936]

12. O'Neill EE, Matallanas D, Kolch W. Mammalian sterile 20-like kinases in tumor suppression: an emerging pathway. Cancer Res. 2005; 65(13):5485–5487. [PubMed: 15994916]

13. Ling P, Lu TJ, Yuan CJ, Lai MD. Biosignaling of mammalian Ste20-related kinases. Cell Signal. 2008; 20(7):1237–1247. [PubMed: 18255267]

14. Cheung WL, Ajiro K, Samejima K, et al. Apoptotic phosphorylation of histone H2B is mediated by mammalian sterile twenty kinase. Cell. 2003; 113(4):507–517. [PubMed: 12757711]

15. Yuan Z, Lehtinen MK, Merlo P, Villen J, Gygi S, Bonni A. Regulation of neuronal cell death by MST1-FOXO1 signaling. J Biol Chem. 2009; 284(17):11285–11292. [PubMed: 19221179]

16. Kerdiles YM, Beisner DR, Tinoco R, et al. Foxo1 links homing and survival of naive T cells by regulating L-selectin, CCR7 and interleukin 7 receptor. Nat Immunol. 2009; 10(2):176–184. [PubMed: 19136962]

17. Ouyang W, Beckett O, Flavell RA, Li MO. An essential role of the Forkhead-box transcription factor Foxo1 in control of T cell homeostasis and tolerance. Immunity. 2009; 30(3):358–371. [PubMed: 19285438]

18. Carlson CM, Endrizzi BT, Wu J, et al. Kruppel-like factor 2 regulates thymocyte and T-cell migration. Nature. 2006; 442(7100):299–302. [PubMed: 16855590]

19. Fabre S, Carrette F, Chen J, et al. FOXO1 regulates L-Selectin and a network of human T cell homing molecules downstream of phosphatidylinositol 3-kinase. J Immunol. 2008; 181(5):2980–2989. [PubMed: 18713968]

20. Lee SK, Surh CD. Role of interleukin-7 in bone and T-cell homeostasis. Immunol Rev. 2005; 208:169–180. [PubMed: 16313348]

21. Schneider M. A cardiac Non proliferative Traety. Science. 2011; 332:426–427. [PubMed: 21512022]

22. Oh S, Lee D, Kim T, et al. Crucial role for Mst1 and Mst2 kinases in early embryonic development of the mouse. Mol Cell Biol. 2009; 29(23):6309–6320. [PubMed: 19786569]

23. Dan I, Watanabe NM, Kusumi A. The Ste20 group kinases as regulators of MAP kinase cascades. Trends Cell Biol. 2001; 11(5):220–230. [PubMed: 11316611]

24. Pan D. The hippo signaling pathway in development and cancer. Dev Cell. 2010; 19(4):491–505. [PubMed: 20951342]

25. McNeill H, Sudol M, Halder G, Strano S, Blandino G, Shaul Y. The Hippo tumor suppressor pathway: a report on the second workshop on the Hippo tumor suppressor pathway. Cell Death Differ. 2011; 18(8):1388–1390. [PubMed: 21566666]

26. Wu S, Huang J, Dong J, Pan D. hippo encodes a Ste-20 family protein kinase that restricts cell proliferation and promotes apoptosis in conjunction with salvador and warts. Cell. 2003; 114(4):445–456. [PubMed: 12941273]

27. Lee KK, Ohyama T, Yajima N, Tsubuki S, Yonehara S. MST, a physiological caspase substrate, highly sensitizes apoptosis both upstream and downstream of caspase activation. J Biol Chem. 2001; 276(22):19276–19285. [PubMed: 11278283]

28. Oh HJ, Lee KK, Song SJ, et al. Role of the tumor suppressor RASSF1A in Mst1-mediated apoptosis. Cancer Res. 2006; 66(5):2562–2569. [PubMed: 16510573]

29. Graves JD, Draves KE, Gotoh Y, Krebs EG, Clark EA. Both phosphorylation and caspase-mediated cleavage contribute to regulation of the Ste20-like protein kinase Mst1 during CD95/Fas-induced apoptosis. J Biol Chem. 2001; 276(18):14909–14915. [PubMed: 11278782]

30. Ahn SH, Cheung WL, Hsu JY, Diaz RL, Smith MM, Allis CD. Sterile 20 kinase phosphorylates histone H2B at serine 10 during hydrogen peroxide-induced apoptosis in S. cerevisiae. Cell. 2005; 120(1):25–36. [PubMed: 15652479]

31. Choi J, Oh S, Lee D, et al. Mst1-FoxO signaling protects Naive T lymphocytes from cellular oxidative stress in mice. PLoS One. 2009; 4(11):e8011. [PubMed: 19956688]

32. Katagiri K, Katakai T, Ebisuno Y, Ueda Y, Okada T, Kinashi T. Mst1 controls lymphocyte trafficking and interstitial motility within lymph nodes. EMBO J. 2009; 28(9):1319–1331. [PubMed: 19339990]

33. Greer EL, Brunet A. FOXO transcription factors at the interface between longevity and tumor suppression. Oncogene. 2005; 24(50):7410–7425. [PubMed: 16288288]

34. Ouyang W, Li MO. Foxo: in command of T lymphocyte homeostasis and tolerance. Trends Immunol. 2011; 32(1):26–33. [PubMed: 21106439]

35. Chen G, Shankar P, Lange C, et al. CD8 T cells specific for human immunodeficiency virus, Epstein-Barr virus, and cytomegalovirus lack molecules for homing to lymphoid sites of infection. Blood. 2001; 98(1):156–164. [PubMed: 11418475]

36. Papagno L, Spina CA, Marchant A, et al. Immune activation and CD8+ T-cell differentiation towards senescence in HIV-1 infection. PLoS Biol. 2004; 2(2):E20. [PubMed: 14966528]

37. Feng X, Wang H, Takata H, Day TJ, Willen J, Hu H. Transcription factor Foxp1 exerts essential cell-intrinsic regulation of the quiescence of naive T cells. Nat Immunol. 2011; 12(6):544–550. [PubMed: 21532575]

38. Nemoto S, Finkel T. Redox regulation of forkhead proteins through a p66shc-dependent signaling pathway. Science. 2002; 295(5564):2450–2452. [PubMed: 11884717]

39. Kops GJ, Dansen TB, Polderman PE, et al. Forkhead transcription factor FOXO3a protects quiescent cells from oxidative stress. Nature. 2002; 419(6904):316–321. [PubMed: 12239572]

40. Notarangelo LD. PIDs and cancer: an evolving story. Blood. 2010; 116(8):1189–1190. [PubMed: 20798238]

41. Grulich AE, van Leeuwen MT, Falster MO, Vajdic CM. Incidence of cancers in people with HIV/AIDS compared with immunosuppressed transplant recipients: a meta-analysis. Lancet. 2007; 370(9581):59–67. [PubMed: 17617273]

42. Feske S. ORAI1 and STIM1 deficiency in human and mice: roles of store-operated Ca2+ entry in the immune system and beyond. Immunol Rev. 2009; 231(1):189–209. [PubMed: 19754898]

43. Engelhardt KR, McGhee S, Winkler S, et al. Large deletions and point mutations involving the dedicator of cytokinesis 8 (DOCK8) in the autosomal-recessive form of hyper-IgE syndrome. J Allergy Clin Immunol. 2009; 124(6):1289–1302. e1284. [PubMed: 20004785]

44. Randall KL, Lambe T, Johnson AL, et al. Dock8 mutations cripple B cell immunological synapses, germinal centers and long-lived antibody production. Nat Immunol. 2009; 10(12):1283–1291. [PubMed: 19898472]

45. Randall KL, Chan SS, Ma CS, et al. DOCK8 deficiency impairs CD8 T cell survival and function in humans and mice. J Exp Med. 2011; 208(11):2305–2320. [PubMed: 22006977]
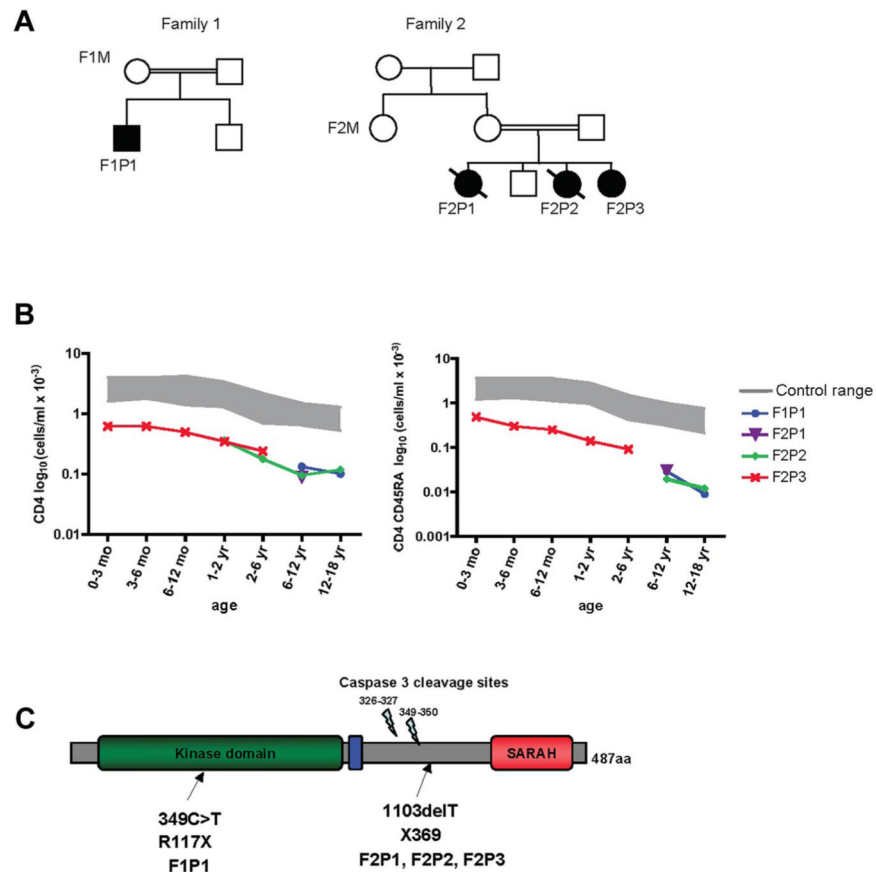
Figure 1. *MST1* mutations in 2 families
(A) Pedigrees of 2 families presenting a CID syndrome. Consanguinity is indicated by double horizontal bars. Black boxes and circles represent affected males and females, respectively. Diagonal bar indicates deceased subjects. An identification number was assigned to each patient. (B) Semilogarithmic graph representing the progressive CD4 T-cell lymphopenia (left) and the marked loss over time of naive CD4 CD45RA^{+} T cells (right) observed in MST1-deficient patients. (C) Schematic representation of the MST1 protein. Mutations identified in the families are indicated by arrows.
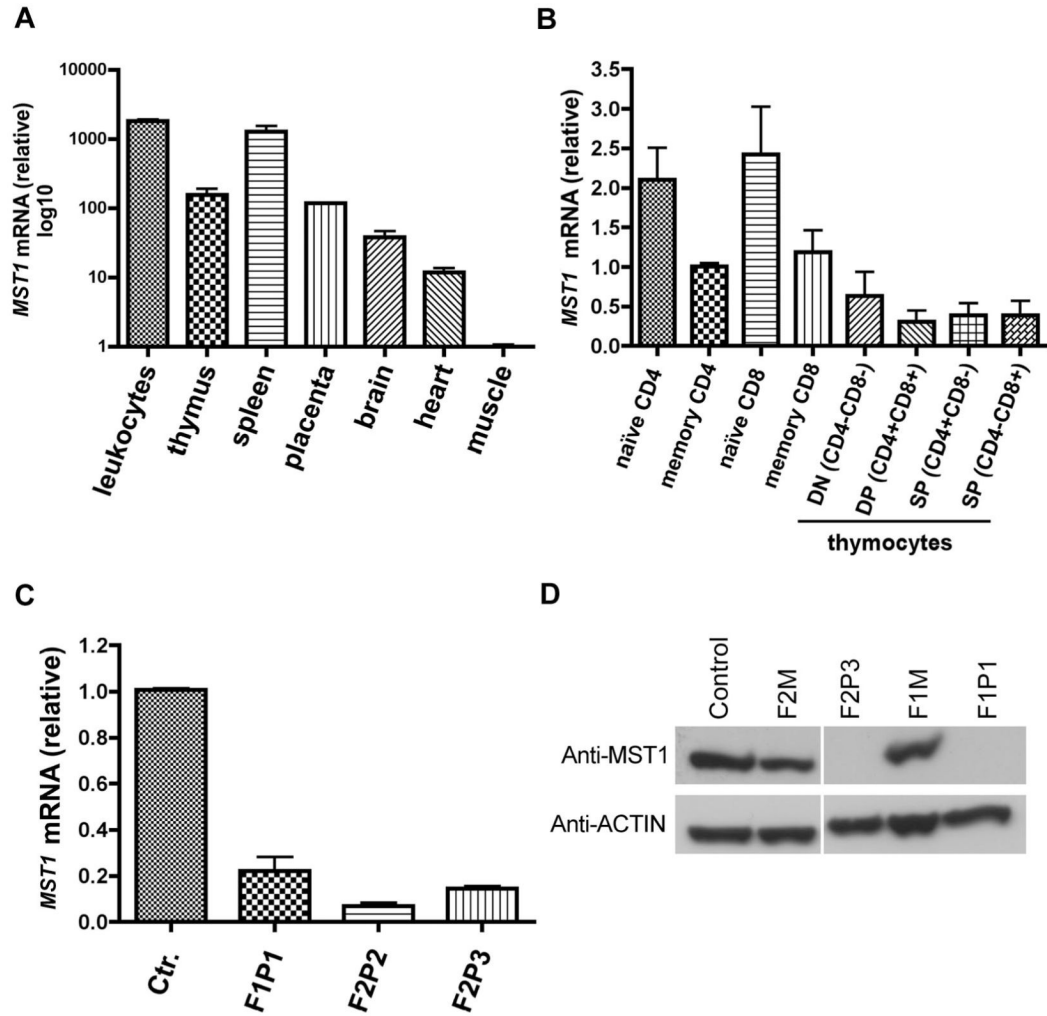
Figure 2. MST1 expression
(A) *MST1* transcript levels were quantified as the -fold difference of mRNA levels for *MST1* normalized against the housekeeping gene *ACTA1* (-actin). Data are representative of 2 independent experiments performed in duplicate. (B) *MST1* transcript levels were quantified as the -fold difference in mRNA levels for *MST1* (normalized to *ACTA1*) in control sorted naive (CD4^{+} CD45RA^{+}; CD8^{+} CD45RA^{+} CCR7^{+}) and memory subpopulations of CD4 (CD4^{+} CD45RO^{+}) and CD8 (CD8^{+} CD45RO^{+} CCR7^{−}) T cells, as well as double-negative, double-positive, and single-positive thymocytes. Data are representative of 3 independent experiments performed in duplicate. (C) *MST1* transcript levels in control and patient T cells. Data are representative of 5 independent experiments performed in duplicate. (D) A Western blot analysis of MST1 protein expression in lymphocytes from a healthy control, 2 heterozygous individuals (F2M, F1M), and 2 MST1-deficient patients with different homozygous nonsense mutations. Actin was used as the loading control. Data are representative of 5 independent experiments.
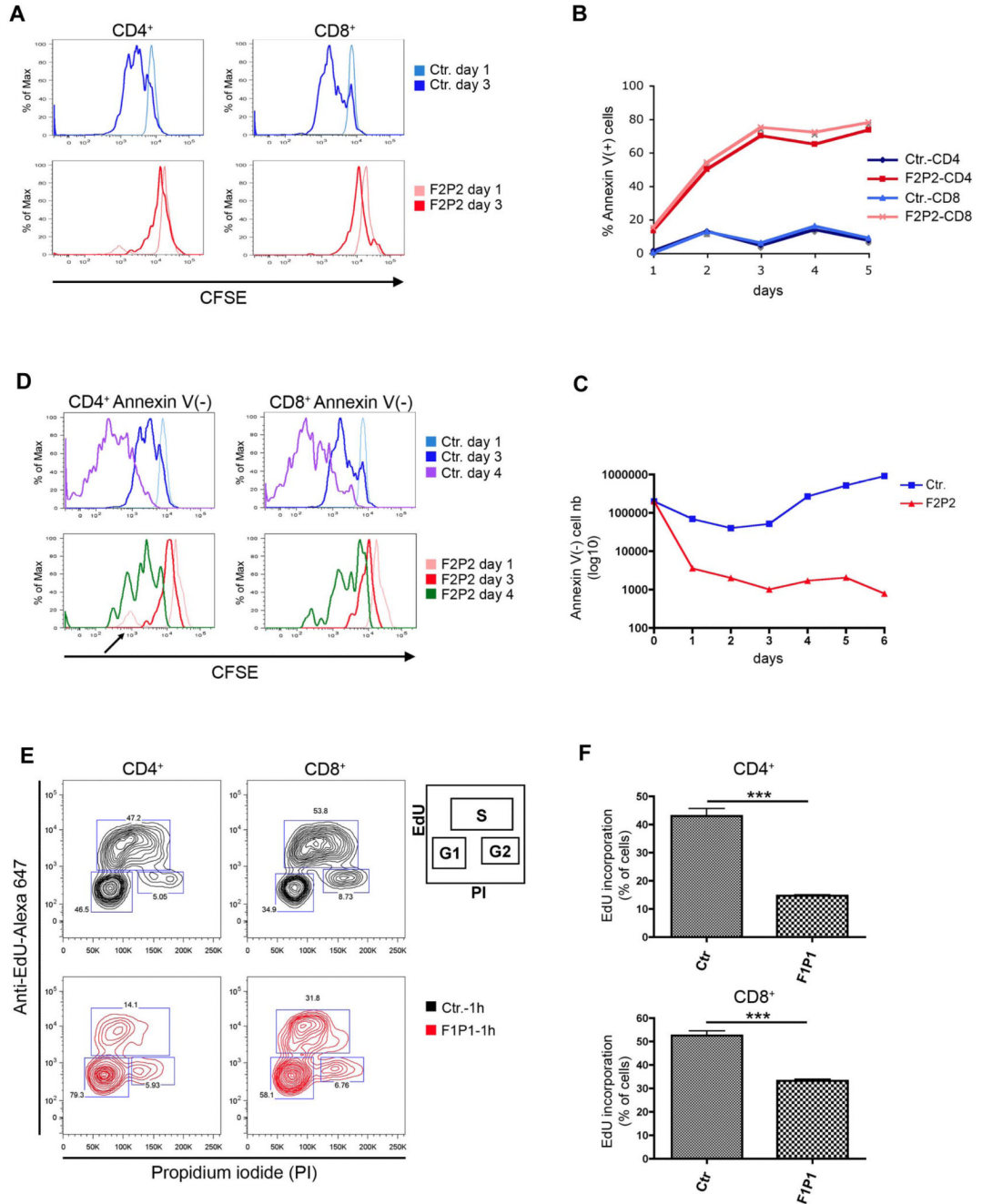
Figure 3. Impaired proliferation and survival of MST1-deficient T cells in response to activation signals

(A) Control (Ctr.) and MST1-deficient (F2P2) CD4 and CD8 T cells were analyzed in terms of the rate of division (with CFSE dilution indicating cell proliferation) every 24 hours from day 1-3 after PMA/ionomycin–induced activation. Data are representative of 4 independent experiments. (B) Cell death, as analyzed by annexin V binding to control (Ctr.) and MST1-deficient (F2P2) CD4 and CD8 T cells, at different time points (every 24 hours) after CFSE labeling and PMA/ionomycin activation. Data are representative of 2 independent experiments. (C) Absolute cell counts for annexin V$^+$ T cells in the CFSE$^+$ population presented in panel B. Data are representative of 3 independent experiments. (D) CFSE and

annexin V staining of PMA/ionomycin-activated control (Ctr.) and MST1-deficient (F2P2) CD4 and CD8 T cells. Cells were stained with annexin V and sized at different time points by flow cytometry. Histograms depict the CFSE dilution of viable CD4 and CD8 T cells (annexin V⁻). It is important to note that the CFSE graphs are normalized against the number of cells; the histograms represent thepercentage of the maximum signal (% of Max) and do not reflect the number of dividing cells. Data are representative of 2 independent experiments. (E) Cell proliferation, as measured by EdU incorporation in control (Ctr.) and MST1-deficient (F1P1) CD4 and CD8 T cells after 8 days of culture. Cells were labeled with EdU for 60 minutes before fixation. The EdU intensity is shown on the logarithmic y-axis and DNA content (propidium iodide staining) is shown on the linear x-axis. Gates defined the percentage of cells in the G_1, S (EdU positive), and G_2 phases, as presented in the inset. Data are representative of 3 independent experiments. (F) Quantification of EdU incorporation by CD4 and CD8 obtained from control (Ctr.) and MST1-deficient patients (F1P1). Data are representative of 3 independent experiments and are shown as means ± SEM. ***P < .001.
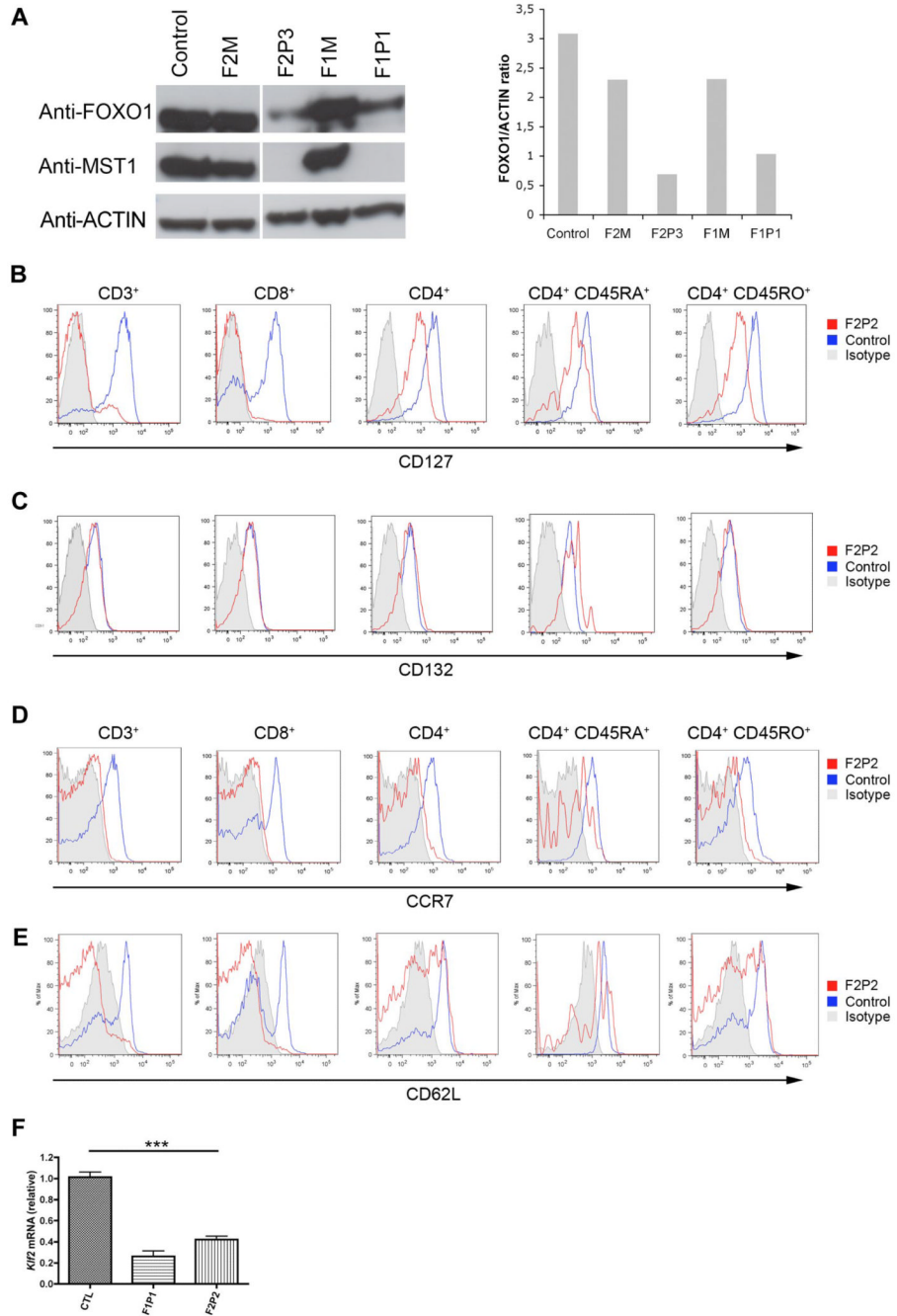
Figure 4. Down-regulation of FOXO1, IL-7Rα, CCR7, and CD62L expression in MST1-deficient T cells

(A) Left: Western blot showing FOXO1 and MST1 protein level in whole-lymphocyte lysates from a healthy control, 2 heterozygous patients (patients F2M and F1M), and 2 MST1-deficient patients with different homozygous nonsense mutations (patients F1P1 and F2P3). Actin served as a loading control. Right: Abundance of FOXO1 relative to actin (signal intensity measurement). Results are presented as the FOXO1/actin ratio (in arbitrary units). Data are representative of 3 independent experiments. (B-C) IL-7Rα (CD127) and common cytokine receptor γ-chain (CD132) expression on CD3, CD8, CD4, CD4 CD45RA^{+}, and CD4 CD45RO^{+} T cells from a control and an MST1-deficient patient

(F2P2). Similar results were obtained for cells from F1P1. One of 6 experiments with similar results is shown (4 independent experiments for F2P2 and 2 for F1P1). (D-E) CCR7 and CD62L expression by freshly isolated control and MST1-deficient (F2P2) PBMCs. One of 6 experiments with similar results is shown (4 independent experiments for F2P2 and 2 for F1P1). (F) Quantitative PCR analysis of *KLF2* mRNA expression. *KLF2* transcript levels were quantified as the -fold difference normalized against *ACTA1* (-actin) mRNA levels in control (Ctr.) and MST1-deficient (F1P1 and F2P2) PBMCs.
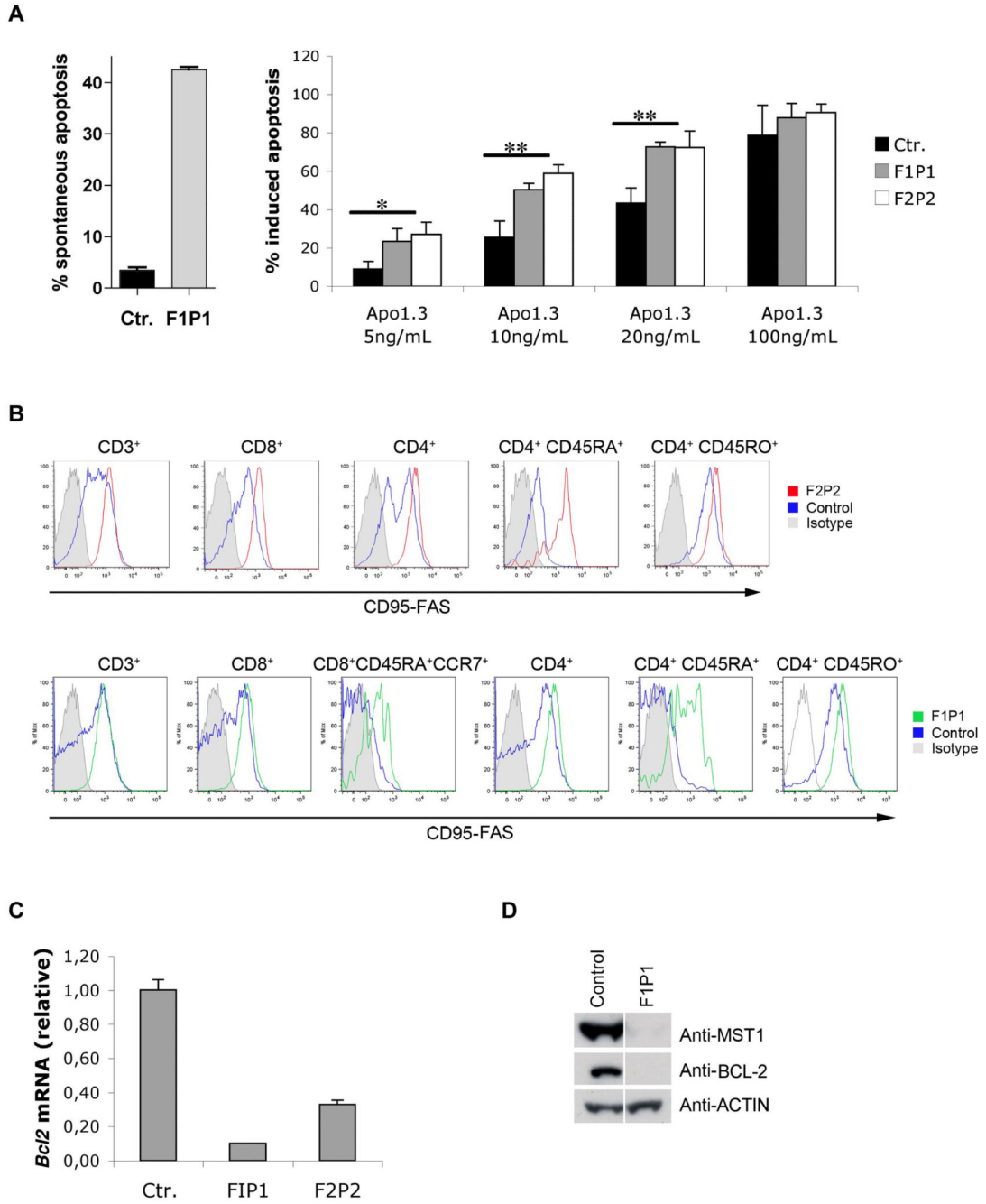
A

B

C

D

Figure 5. Greater expression of FAS is correlated with greater sensitivity to FAS-induced apoptosis and down-regulation of BCL2 expression in MST1-deficient T cells

(A) Spontaneous apoptosis (left) and death-receptor-induced apoptosis (right) in vitro was assessed on PMA/ionomycin-activated T cells from control (Ctr.) and MST1-deficient patients (patients F1P1 and F2P2). After 8 days of activation, blasts were incubated overnight in the absence or presence of a dose gradient of anti-FAS Ab (Apo1.3). The percentage of apoptotic cells (means ± SEM of 3 independent experiments) was then measured by propidium iodide labeling of DNA fragmentation. *P< .05; **P< .01. (B) FAS expression on PBMCs freshly isolated from control (Ctr.) and MST1-deficient patients (patients F1P1 and F2P2). FAS expression was monitored in a freshly isolated T-cell

subpopulation. One of 6 experiments with similar results is shown. (C) Quantitative PCR analysis of *BCL2* mRNA expression normalized against *ACTA1* (-actin) mRNA in total PBMCs freshly isolated from control (Ctr.) and MST1-deficient patients (patients F1P1 and F2P2). Data represent the means of 4 independent experiments. (D) Western blot showing BCL2 and MST1 protein levels in whole lymphocytes lysates from a healthy individual and an MST1-deficient patient (patient F1P1). Actin served as the loading control.

Table 1
Immunological characteristics of patients F1P1, F2P1, F2P2, and F2P3

	F1P1	F2P1	F2P2	F2P3
Age, y	16	9	11	3
Lymphocytes, /μL × 10⁻³ (normal range)	0.7 (1.4-3.3)	0.9 (1.9-3.7)	1.5 (1.9-3.7)	1.6 (2.3-5.4)
T-cell population (normal range)				
CD3⁺, /μL × 10⁻³	0.52 (1.0-2.2)	0.40 (1.2-2.6)	1.4 (1.2-2.6)	0.54 (1.4-3.7)
TCR /CD3⁺, % (92-98)	54	99	87	94
TCR /CD3⁺, % (2-8)	46	0.3	13	6
CD4⁺, /μL × 10⁻³	0.13 (0.53-1.30)	0.10 (0.60-1.50)	0.16 (0.60-1.50)	0.24 (0.70-2.20)
CD8⁺, /μL × 10⁻³	0.20 (0.33-0.92)	0.41 (0.37-1.10)	1.23 (0.37-1.10)	0.26 (0.49-1.30)
CD31⁺CD45RA⁺/CD4⁺, %	1 (42-55)	2 (42-74)	2 (42-74)	31 (50-85)
Regulatory T cell CD4⁺CD25⁺⁺, /μL	4 (16-40) *	ND	11 (80-130) †	37 (80-130) †
CD45RA⁺/CD8⁺, %	51 (61-91)	36 (63-92)	86 (63-92)	94 (69-97)
CD45RA⁺CCR7⁺/CD8⁺, %	1.3 (52-68)	1 (52-68)	ND	ND
CD45RA⁺CCR7⁻/CD8⁺, %	18 (16-28)	80 (16-28)	ND	ND
HLA-Class-II/CD3⁺ 10, %	49‡	ND	46‡	ND
T-cell proliferation, cpm × 10⁻³ to:				
Phytohemagglutinin (n > 50)	4	ND	7	8
Anti-CD3 Ab (n > 30)	ND	0	5	13
PMA + ionomycin + IL2 (n > 80)	12	ND	10	22
Candida Ag (n > 10)	0.8	0.8	ND	16.5
Tetanus toxoid (n > 10)	1	0.6	ND	19
Varicella zoster virus (n > 10)	ND	1.1	3.6	ND
B-cell population				
B-lymphocyte (CD19⁺), /μL × 10⁻³ (normal range)	0§ (0.11-0.57)	0.42 (0.27-0.86)	0.03 (0.27-0.86)	0.60 (0.39-1.40)
CD27⁺/CD19⁺ memory, %	ND	1 (> 10)	13 (> 10)	ND
Natural killer cells (normal range)				
CD56⁺CD16⁺ per μL × 10⁻³	0.17 (0.10-0.48)	0.36 (0.10-0.48)	0.3 (0.10-0.48)	0.42 (0.13-0.72)
Ig levels, mg/mL (normal range)				
IgM	0.37 (0.55-1.77)	< 0.17 (10.68-1.28)	0.74 (0.54-1.53)	0.73 (0.54-1.53)
IgG	22.6 (4.8-14.)	20.5 (8.3-14.3)	15 (5.5-10.2)	14.3 (5.5-10)
IgA	2.19 (0.49-1.90)	10.9 (1.02-1.94)	3.24 (0.41-1.41)	1.74 (0.41-1.41)
IgE, U/mL	110 (10-100)	12 (10-100)	ND	ND
Allo-hemagglutinins titer IgG	1:32 (> 1:16)	ND	1:4 (> 1:16)	1:256 (> 1:16)
Abs following immunization (normal range)				
Anti-polio titer, × 10⁻¹ (40)	80/160/40	80/40/320	> 1280/64/64	ND
Anti-diphtheria toxoid, IU/mL(1)	< 0.1	ND	ND	ND

	F1P1	F2P1	F2P2	F2P3
Anti-tetanus toxoid, IU/mL (0.5)	0.16[¶]	ND	ND	ND
Anti–*Haemophilus influenzae* (3 μg/mL)	< 0.1	< 0.1[¶]	ND	ND
Anti–*Streptococcus pneumoniae* (> 3 μg/mL)	ND	< 3[¶]	< 3[¶]	ND

ND indicates not determined.

[*] CD127 low, CD25 high, CD4.

[†] CD25 high, CD4.

[‡] Moderate expression

[§] After anti-CD20 therapy.

[¶] Three months after vaccination in F1P1 and 6 weeks after vaccination plus previous infection in F2P1 and F2P2.